REVISTA MATÉRIA V.29 N.1
ISSN 1517-7076 articles e20230322, 2024

Evaluation of machinability performance of T51603 using response surface methodology and grey relational analysis

R. Suresh Kumar[1], S. Vinodh[2], P. Satishkumar[3], S. Seenivasan[3]

[1]Sri Eshwar College of Engineering, Department of Mechanical Engineering, Centre for Advanced Materials & Testing. Coimbatore, Tamil Nadu, India.

[2]Sri Eshwar College of Engineering, Department of Mechanical Engineering. Coimbatore, Tamil Nadu, India.

[3]Rathinam Technical Campus, Department of Mechanical Engineering. Coimbatore, Tamil Nadu, India.

e-mail: rsureshkumarsece@gmail.com, vino.infomech@gmail.com, sp.sathishkumar10@gmail.com, seenikct@gmail.com

ABSTRACT

The goal of this study is to increase material removal rate (M_{rr}), and minimize consumption of power (P_c) and surface integrity (S_r) while using the least amount of resources thereby addressing sustainable manufacturing and optimization in machining operation. Box Behnken Design (BBD) and Grey Regression Analysis (GRA) are systematically followed in the machining process on UNS T51603. The experimental runs were performed based on BBD followed by multi-objective optimization using GRA. The practical applicability and reliability of the optimized parameters is evaluated by confirmatory runs, and the optimal solution of single and multi-objective solution for S_r, M_{rr}, and P_c, is verified. The lowest S_r was achieved when S_s was maintained at 2000 rpm, with D_c at 0.6 mm, F_r at 750 mm/min, and C_{fr} 6 l/min. maximum M_{rr} was attained when S_s assigned at 1750 rpm, with D_c at 0.6 mm, F_r at 750 mm/min, and C_{fr} 8 l/min. When compared to confirmatory runs, the optimized set of parameters for BBD and GRA reveals a 10% variance, demonstrating the validity of the optimization strategies used. In terms of P_c the optimized parameters were found to be 1750 rpm, 0.2 mm, 500 mm/min, and 6 l/min.

Keywords: CNC end milling; Grey regression analysis; Box Behnken; Surface roughness; Material removal rate.

1. INTRODUCTION

CNC machining has established an unbeatable position in recent years by providing improved dependability, accuracy, and productivity. Additionally, CNC milling offers greater freedom in selecting the levels of the cutting parameters. Various milling procedures are used in industries. Out of these, the CNC end milling technique is unavoidable in the automotive, aerospace, and metal processing industries as it delivers high precision, accuracy, and dependability. End milling attained an unrivalled position in the manufacturing industry by meeting demands. Numerous criteria that regulate the process are included in every machining operation. Both controllable and non-controllable characteristics fall under this category. S_s, C_s, F_r, D_c, and other variables are examples of controllable parameters that can be adjusted in accordance with requirements. Non-controllable parameters are those that can be regulated indirectly by controllable parameters rather than being directly controlled. A few examples include chip formation vibrations, tool wear (T_w), and S_r.

Surface integrity was the subject of an experimental research on Al2014-T6 by WANG and CHANG *et al.* [1]. Slot end milling was used for trial runs. The study found that the main determinants of S_r are vibrations during milling and the F_r. PALANISAMY *et al.* [2] analyzed the parameter effect of CNC milling and proposed optimum settings. The study used a genetic algorithm, and the experimental analysis proved that F_r and D_c played significant role in governing S_r. MUTHUKRISHNAN and DAVIM [3] conducted an extensive study in adaptive control of CNC machining. The development of research into maintaining the precision and dependability of machining parameters was thoroughly covered in this study. The article provided a summary of the methods created thus far to increase the effectiveness of CNC machining. QUINTANA *et al.* [4] provided a strategy for surface integrity prediction. The study was limited to one objective function, and potential consequences of other responses were not taken into account. MANSOUR and ABDALLA [5] created an analytical model.

Corresponding Author: R. Suresh Kumar Received on 18/11/2023 Accepted on 06/02/2024

DOI: https://doi.org/10.1590/1517-7076-RMAT-2023-0322

SURESH *et al.* [6] studied single-response and multi-response optimization using the Taguchi design and grey relational analysis (GRA) while working on Al6063 using green machining techniques.

The study implicated C_s, F_r, and D_c as the regulating parameters. The optimization exploration employing DOE on S_r was acknowledged by CHANG *et al.* [7]. In a different study, GOLOGLU and SAKARYA [8] and DHOKIA *et al.* [9] employed DOE to forecast the ideal degree of S_r. By utilizing the taguchi based GRA [10], optimization was performed to arrive at minimum corrosion rate and weight loss of Al/SiCp. It was a metal matrix composite experimented as per L9 orthogonal array involving volume % of SiCp, NaCl solution and time factor for determining the effects on corrosion rate and weight loss incurred. The review also sheds light on the sophisticated optimization methods like GA, ANN, and fuzzy [11, 12, 13] to determine the best set of parameters for machining. A study on low-carbon mold steel (UNS T51620) was carried out using BBD and GRA for the optimization of R_a and M_{rr} and P_c. The result showed significant improvement in the optimized set of parameters with a 10% deviation proving the reliability of the developed model [14, 15, 16]. A literature study was exclusively carried [17] on GA and their use in CNC milling for the optimization of machining parameters.

A vivid picture on machining relationship [18] was presented a work based on cloud computing assisting a thorough analysis of cutting tool measurement in the turning process. In this research, the interaction effect between the parameters and responses were studied. A single objective function optimization was performed using GA by OKTEM *et al.* [19] to determine the optimal value for minimizing R_a. SINGH *et al.* [20] used taguchi resilient design to implement a multi-objective strategy for cyclone separator optimization, validated through numerical simulation. In another work ideal tool-stress model for EN8 steel in CNC turning was proposed. One may see substantial research in machining employing higher-order techniques in terms of optimization. However, it is important to remember that the majority of the labour done is restricted to single-objective tasks. In actuality, there are usually several, incongruent responses to any machining operation. As a result, it becomes necessary to interpret the results of parameter interaction effects to arrive at the key machining settings.

Another research was performed on EN8 steel for sustainable manufacturing using multi-criteria decision making (MCDM) approach for optimization of machining parameters [21]. The study focused on optimizing M_{rr}, S_r, noise level and cutting force. The experiments were performed aligned to L27 orthogonal array with controllable parameters as C_s, F_r and D_c. The result showed that the responses were highly influenced by F_r followed by D_c and C_s. A study on the optimization of process parameters was performed by Mian and team for Near Dry Turning (NDT) of two steel grades, EN8 and EN31 [22]. Near Dry Turning was adopted with minimal amount of coolant with a predominant use of compressed air. In this study, Al_2O_3 nanofluid was employed as a coolant along with compressed air. The primary machining parameters investigated were C_s, F_r and D_c, with a focus on achieving efficient cooling. The result showed a reduction in S_r of 12.3% and 14.6% for EN8 and EN31 in dry machining using nanofluid. Also, the result showed a reduction of 7% temperature in cutting area. These results appealed the significance of optimization and recommended the used nanofluid in near dry turning of steels.

A detailed review [23] was carried out on cutting fluids and their methods of application during various machining operations. The review also consolidated issues associated with conventional and concerned sustainability metrics. Precisely, techniques like dry machining, minimum quantity cooling and lubrication, gas based coolant, solid lubricants, cryogenic means provided superior machinability compared to conventional means. The review also summarized demands and challenges involved in sustainability techniques.

1.1. Literature gap identified

The extensive literature survey performed gave an insight towards tool steel where only few research has been performed. Tool steel is a type of high-quality carbon and alloy steel that is specifically designed for the production of tools and dies. These steels are engineered to have the necessary properties for cutting, shaping, and forming materials in various industrial processes. Tool steels are known for their exceptional hardness, wear resistance, and toughness. They are hardened to withstand the repeated impacts and stresses encountered in cutting, forming, and shaping operations. They can be heat-treated to achieve high levels of hardness. Resistance towards wear, abrasion, and deformation is very crucial for maintaining sharp cutting edges and prolonging the life of the tool. These steels are specifically designed for use in mold and die applications where good machinability, weldability, and surface finish are essential.

SAE-AISI P3 steel also known as UNS T51603 is suitable for higher stress applications like stamping, forging and cutting as it offers best suited combination of. The superior qualities in terms of resistance to wear, toughness, and hardness makes it unique in such applications. Moreover, these steels are highly stable to deformation and cracking when subjected to heat treatment processes. T51603 finds its applications in almost all industries requiring higher precision and dependability. Since this material is universally used in varied industry applications, the need to provide machinability solutions towards sustainability is inevitable. From literature survey, it is also found that few research was performed in T51603 addressing towards optimization and sustainability. The proposed work is a single and multi-objective function, and an attempt towards optimizing three seemingly incongruent responses: S_r, M_{rr}, and P_c while machining Low-Carbon Mold Steel UNS T51603. This study involves application of BBD for performing the experimental runs followed by arriving at the optimized parameters through multi-objective optimization involving contradictory responses using GRA. The application of BBD and GRA in the study of T51603 is unique as no previous research has been made in this segment.

2. METHODOLOGY AND IMPLEMENTATION

2.1. Work material and tool

The primary alloying components, viz. nickel and chromium dominant the low-carbon mold steels, which are categorized as group P steels. For these steels to develop the desired properties, nitriding or carburizing is typically used. Due to their ease of machining into intricate and substantial molds and dies, these steels have good machinability. They are mostly utilized in die casting and injection molds. Pre-hardened UNS T51603 steel is chosen as the work material due to its broad application. The hardness of the work material is determined in the laboratory using Brinell Hardness Testing Machine and found to be 341 HB. For machining, a rectangular work piece with the following measurements is used: 75×30×12 (dimensions in mm). The chemical constituents of the work material are evaluated in SITARC (Scientific and Industrial Testing and Research Center), Coimbatore and is shown in Table 1. The selected material finds its applications in clinching fasteners, studs, nuts, bolt, screws etc.

2.2. Controllable & non-controllable parameters

The S_s, F_r, D_c, tool rake angle (T_{ra}), C_{fr}, S_r, L_t, etc., all have a significant impact on machining operations [24, 25]. Out of them, some parameters, known as controllable parameters can be managed prior to the execution of machining. Uncontrollable parameters are those which are indirectly controlled through controllable parameters like S_r, M_{rr}, P_c etc. The present study involves S_s, D_c, F_r, and C_{fr} as the controllable parameters. The uncontrollable parameters or responses are S_r, M_{rr}, and P_c. The levels of the chosen adjustable parameters are set in accordance with the manufacturer's recommendations and current research. The F_r (mm/min), S_s (rpm), D_c (mm), and C_{fr} (l/min) are the controllable parameters that have been recognized and taken into account. The experiments were performed in a 3-axis vertical milling center and the sample are machined as per the design matrix shown in Figure 1. The bed size of the machine used was 700 × 400 mm, with X, Y, Z travel of 700 mm/min, 400 mm/min

Table 1: Chemical constituents (wt %).

Ni	Si	C	Mn	S	P	Cr
1.2	0.39	0.10	0.58	0.02	0.03	0.48

Figure 1: Runs conducted.

Figure 2: Surface roughness testing.

and 300 mm/min respectively. The maximum spindle speed of the machine was restricted to 16,000 rpm. The machined surface is evaluated using surface testing equipment of MITUTOYO brand with resolution between 0.01 µm to 0.3 µm. The Sr was measured in three different locations and the average value was taken for further analysis as shown in Figure 2.

2.3. Scanning Electron Microscope (SEM)

SEM analysis for machinability studies provides detailed insights into the microstructure and behavior of materials during the machining process for optimizing cutting parameters and study the pattern of machined surface. Following are the specifications maintained for SEM analysis:

1. Sample dimension: The machined samples were prepared for SEM analysis with a dimension of 10 × 10 × 10 mm.
2. Electron High Tension (EHT): The EHT was maintained at 5.00 kV.
3. Working Distance (WD): WD was maintained a1 11.0 mm.
4. Signal: Secondary signal (SE) was taken up for the analysis.
5. Magnifications used: 100×, 250×, 500×, 1000×.

2.4. Design matrix

Table 2 highlights the factors and levels assigned for each parameters. The runs were performed as per BBD sequences as shown in Table 3 with responses measured.

Table 2: Factors and levels.

PARAMETERS	LEVELS		
	1	2	3
S_s(rpm)	1500	1750	2000
D_c(mm)	0.2	0.4	0.6
F_r(mm/min)	500	750	1000
C_{fr}(l/min)	4	6	8

Table 3: Design matrix.

RUN ORDER	S_s (rpm)	D_c (mm)	F_r (mm/min)	C_{fr} (l/min)	S_r (µm)	M_{rr} (IPM)	P_c (HP)
1	1750	0.6	500	6	2.887	1.2111	1.131
2	1750	0.2	750	4	4.636	0.1944	0.251
3	1750	0.4	750	6	3.424	0.7636	0.806
4	2000	0.2	750	6	2.844	0.2171	0.262
5	1500	0.6	750	6	4.004	1.3101	1.349
6	1750	0.4	750	6	3.424	0.7636	0.806
7	1500	0.4	1000	6	4.54	0.8626	1.024
8	2000	0.4	750	8	1.632	0.7863	0.817
9	1500	0.2	750	6	5.324	0.3341	0.423
10	1750	0.4	750	6	3.424	0.7636	0.806
11	1750	0.4	500	8	2.995	0.8043	0.76
12	1750	0.4	500	4	4.099	0.6419	0.576
13	1750	0.6	1000	6	2.64	1.2921	1.406
14	1750	0.4	750	6	3.424	0.7636	0.806
15	1750	0.6	750	4	3.316	1.1704	1.177
16	2000	0.6	750	6	1.524	1.1931	1.188
17	1500	0.4	750	4	5.216	0.7409	0.794
18	2000	0.4	750	4	2.736	0.6239	0.633
19	1750	0.2	750	8	3.532	0.3568	0.435
20	1750	0.2	500	6	4.207	0.2351	0.205
21	2000	0.4	500	6	2.307	0.6646	0.588
22	1750	0.2	1000	6	3.96	0.3161	0.48
23	1750	0.6	750	8	2.212	1.3328	1.361
24	1750	0.4	1000	4	3.852	0.7229	0.851
25	2000	0.4	1000	6	2.06	0.7456	0.863
26	1500	0.4	750	8	4.112	0.9033	0.979
27	1750	0.4	750	6	3.424	0.7636	0.806
28	1750	0.4	1000	8	2.748	0.8853	1.035
29	1500	0.4	500	6	4.787	0.7816	0.749

3. RESULTS AND DISCUSSIONS

The next sections cover each distinct parametric effect on the responses. Based on the desirability function, the machining parameters were optimized. Analysis of Variance (ANOVA) validates the desirability function's competence.

3.1. RSM for S_r

According to the analysis shown above, "F-value" of 627600 and a "P-value" less than 0.0001 adheres to the desirability as enlisted in Table 4. The insignificance of the model arises when the values records more than 0.10. In other words, only 0.01% chance exists that noise will have a negligible influence [12, 26, 27]. Additionally, R^2, Adj R^2, and Pred R^2 values near to 1 justifies the efficiency of the model. The surface graphs presented below provides vivid picture towards interaction between machining parameters and S_r.

Table 4: ANOVA – S_r.

ANOVA- S_r						
SOURCE	**SS**	**DF**	**MS**	**F-VALUE**	**P-VALUE**	
Model	26.83787	14	1.78556	627600.00	<0.0001	significant
S_s	18.6512	1	18.8512	627620.00	<0.0001	
D_c	5.3272	1	5.2272	67590	<0.0001	
F_r	0.193027	1	0.183027	5788618.94	<0.0001	
C_{fr}	3.676448	1	3.656448	1866573.15	<0.0001	
Residual Error	1.58533	14	0			
Lack of Fit	0	10	0			
Pure Error	0	4	0			
Cor Total	27.8178	28				

Standard Deviation	0.0003879	R^2	0.999998
Mean	3.43	Adj R^2	0.999997
C.V.%	0.0833287	Pred R^2	NA

3.1.1. Parameter interaction effects

Figure 3 displays the interaction plot between S_s and D_c on S_r. When level of D_c is assigned between 0.45 to 0.60 mm and S_s is between 1800 to 2500 rpm, the least amount of R_a is produced. Any departure from the aforementioned level had a negative impact on the reaction R_a. Figure 4 depicts the interaction of F_r and C_{fr} on S_r. The graphical view highlights that higher level of C_{fr} aids in getting better S_r. Whereas, in the case of F_r, all levels significantly contributes towards better S_r. However, it also depends on the level assigned for other controllable parameters [13, 28]. When additional parameters are taken into account for measurement, it is discovered that the effect of parameter F_r has the least impact on S_r.

The interaction plot between S_s and C_{fr} on S_r is depicted in Figure 5. The least S_r is achieved when both parameters are maintained at higher levels between 2200 to 2500 rpm and 6 to 8 l/min. When parameter S_s and parameter C_{fr} are steadily increased, better results are obtained.

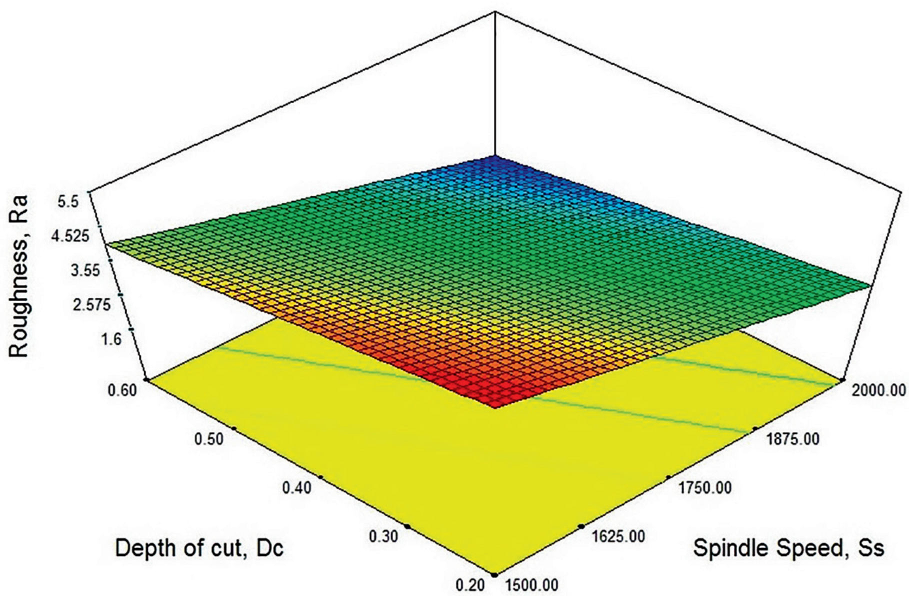

Figure 3: Interaction plot: S_s & D_c on S_r.

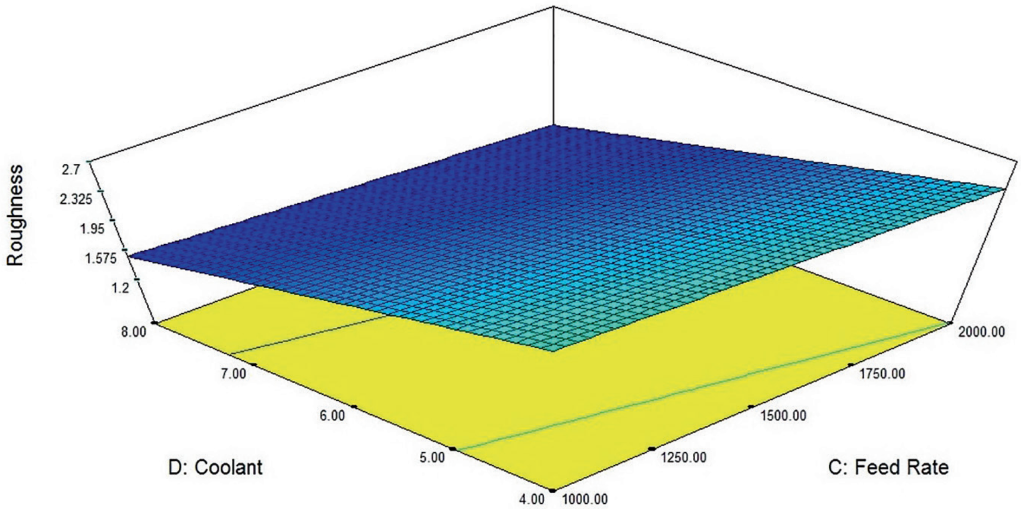

Figure 4: Interaction plot: F_r & C_{fr} on S_r.

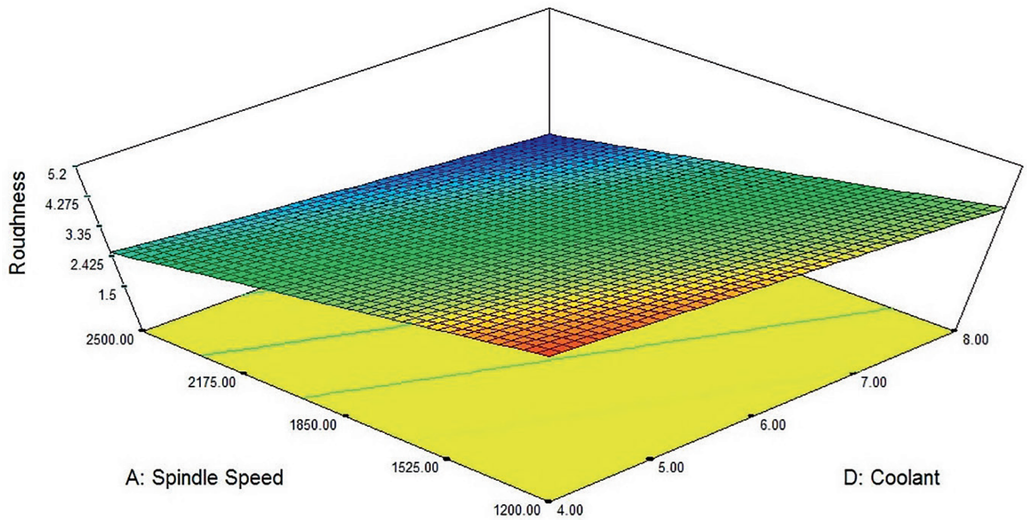

Figure 5: Interaction plot: S_s & C_{fr} on S_r.

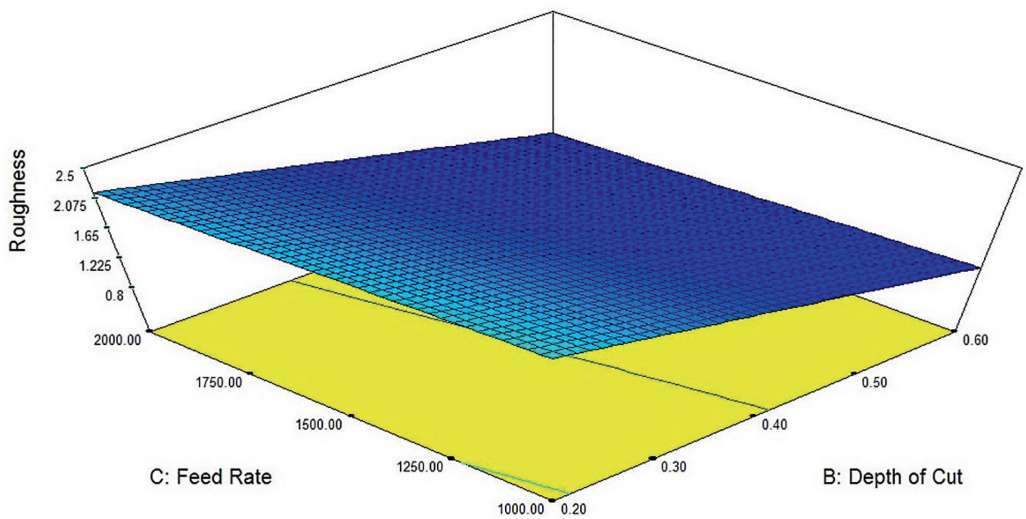

Figure 6: Interaction plot: F_r & D_c on S_r.

The influence between F_r and D_c on S_r is shown in Figure 6. A thorough examination reveals that parameter F_r has a stronger influence on the response S_r than D_c. It may be concluded from trial runs 3 and 6, that lowering the level of F_r lowers the S_r. It is noteworthy to state that when other parameters are maintained at the same level (as observed in runs 3, 6 and 28) the effect of S_s on S_r is higher. This offers a clear picture on the leading parameter impacting S_r. In this instance, the most important parameter impacting S_r are in the following order: S_s, F_r, D_c, and C_{fr}.

3.1.2. Optimized parameters for S_r

The optimized (single response) parameters for S_r is listed in the Table 5. From the experimental analysis though F_r had a much stronger influence on S_r compared to S_s and D_c, for achieving minimum S_r, the best combination was found to be a medium F_r that provided a good balance between chip formation and tool engagement, minimizing tool deflections and chatter that can worsen S_r. Moreover, T51603 steel having specific characteristics makes it less sensitive to S_s and D_c within certain ranges. Additionally, the chosen tool geometry and material might have been particularly well-suited for these higher cutting parameters while maintaining good surface finish.

3.2. RSM for M_{rr}

M_{rr} is calculated theoretically using the relation given below:

$$M_{rr} = D_{c1} \times D_{c2} \times Vf \tag{1}$$

$$Vf = F_z \times n \times Z_{effc} \tag{2}$$

where, D_{c1} is axial depth of cut, D_{c2} is the radial depth of cut, F_z is the feed per tooth, n is the spindle speed and Z_{effc} is the number of effective tooth.

Table 6 highlights the ANOVA for M_{rr}. According to the analysis shown above, F-value of 678091.19 and a P-value less than 0.0001 adheres to the desirability function. The insignificance of the model arises when the values records more than 0.10. In other words, only 0.01% chance exists that noise will have a negligible

Table 5: Optimized parameters – S_r.

D_c	C_{fr}	S_s	F_r	S_r
0.6	6	2000	750	1.524

Table 6: ANOVA – M_{rr}.

ANOVA – M_{rr}						
SOURCE	**SS**	**df**	**MS**	**F-VALUE**	**P-VALUE**	
Model	2.996899	4	0.78969	678091.19	<0.0001	significant
S_s	0.051167	1	0.06126	123432.95	<0.0001	
D_c	2.887748	1	2.88762	769879.27	<0.0001	
F_r	0.029686	1	0.02968	434180.42	<0.0001	
C_{fr}	0.079521	1	0.08962	65660000	<0.0001	
Residual Error	1.88653	24	0			
Lack of Fit	0	20	0			
Pure Error	0	4	0			
Cor Total	2.997699	28				

Standard Deviation	0.0006958	R^2	0.987379
Mean	0.57664	Adj R^2	0.987747
C.V.%	0.0755287	Pred R^2	NA
PRESS	NA	Adequate Precision	2342.5029

influence. Additionally, R^2, Adj R^2, and Pred R^2 values near to 1 justifies the efficiency of the model. The interaction of parameters and M_{rr} is clearly seen in the surface interaction charts that are presented below [29, 30, 31].

3.2.1. Parameter interaction effects

The impact of the parameters on M_{rr} is seen in the interaction graphs below. The interaction effect between S_s and D_c on M_{rr} is depicted in Figure 7. When S_s is assigned with level 1 and D_c is steadily increased (as observed in trial 1, 16, and 17) demonstrate a steady increase in M_{rr}. On the other hand, when S_s is altered and other parameters are maintained at level 1 (5, 11, and 13), one can witness a rise in M_{rr} however, the rate of growth is significantly slower than former condition. This proof validates that F_r is more significant compared to S_s.

Figure 8 illustrates how parameter F_r and D_c have an impact on M_{rr} during machining. When S_s and D_c are kept at 2500 rpm and 0.4 mm, and F_r is steadily increased (runs 4, 5, and 29), a steady raise in M_{rr} can be observed. In contrast, when the levels of S_s and F_r are held constant (1850 rpm, 1500 mm/min) and D_c is changed (runs 8, 9, and 26), D_c showed significant contribution towards rapid increase in M_{rr}. This observation validates the significant role of D_c compared to F_r. The machining impact of C_{fr} and F_r on M_{rr} is depicted in Figure 9. Runs 8, 13, 18, 23, 26, and 28 shows the significant effect of C_{fr} when other parameters are held constant. An increase in M_{rr} can be seen in the experimental runs mentioned above. The use of coolant improves M_{rr} in comparison to F_r, but also depends on D_c and S_s. Figure 10 illustrates how parameters S_s and C_{fr} related to machining affected M_{rr}. When other parameters are held constant, the effects of C_{fr} are clearly shown in the experimental runs 8 and

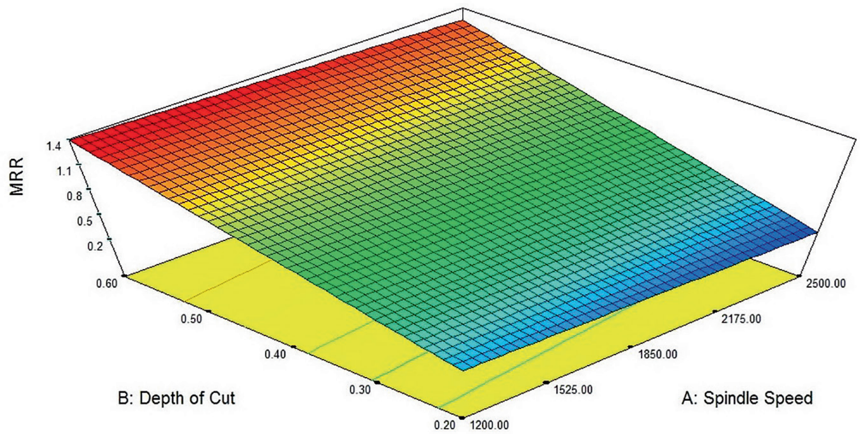

Figure 7: Interaction plot: D_c & S_s on M_{rr}.

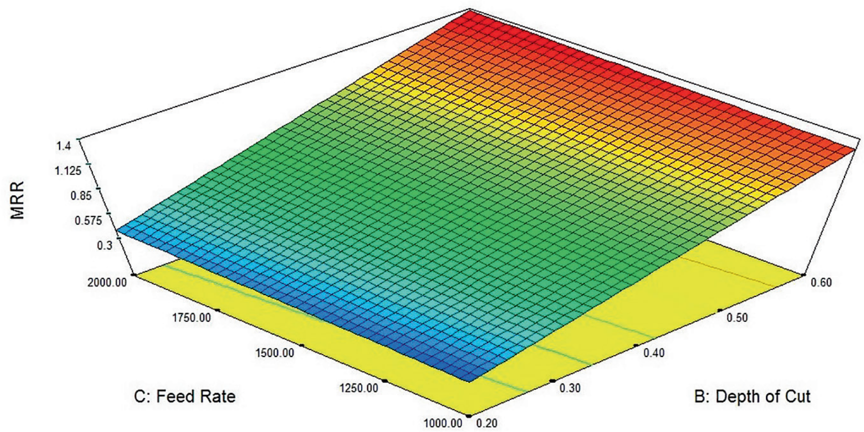

Figure 8: Interaction plot: F_r & D_c on M_{rr}.

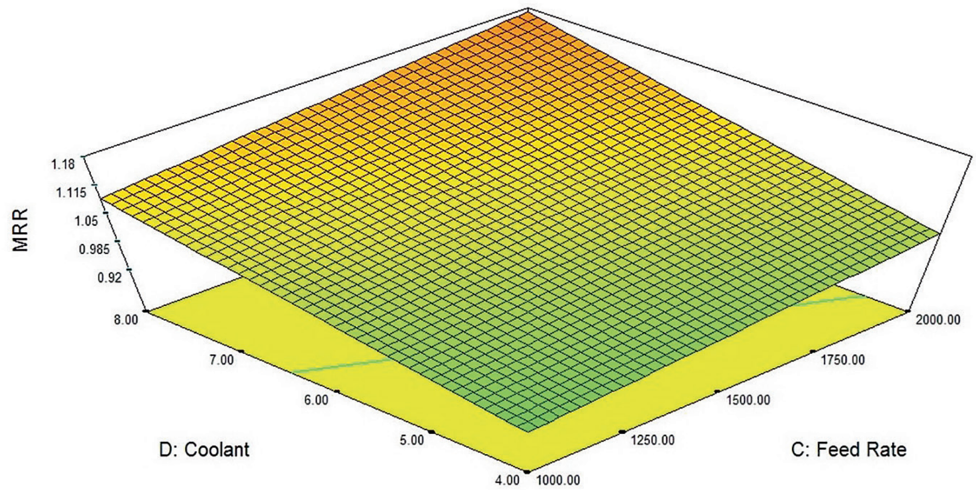

Figure 9: Interaction plot: C_{fr} & F_r on M_{rr}.

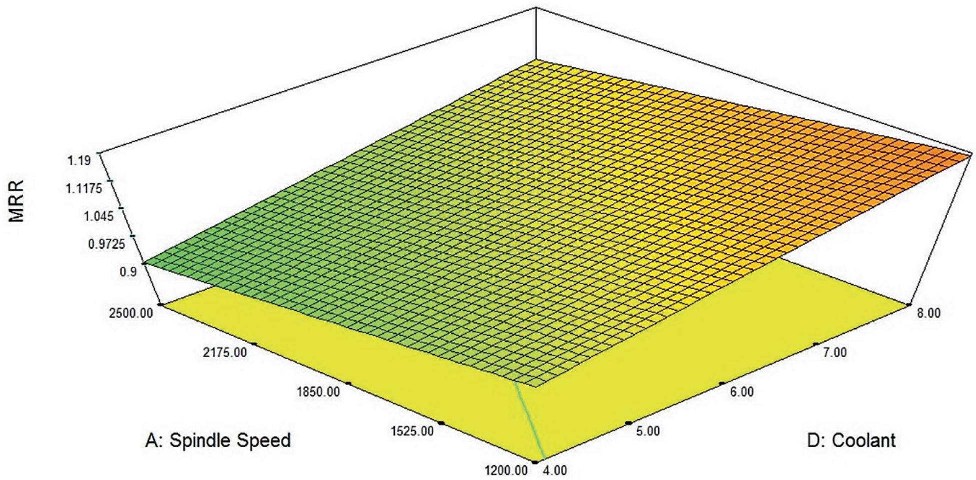

Figure 10: Interaction plot: S_s & C_{fr} on M_{rr}.

13, 18 and 28, 23 and 26, and so on. The M_{rr} has increased in the trial runs mentioned above. On the other hand, when S_s is changed while leaving all other parameters constant, experimental runs 11 & 22, 3 & 29, and 14 & 20 demonstrate an increase in M_{rr}.

3.2.2. Optimized parameters for M_{rr}

The optimized parameters are enlisted in Table 7. The experimental analysis showed that higher D_c had a significantly stronger influence on M_{rr} compared to S_s and F_r. This combination provided the best combination offering least tool wear or deflections that could counteract the depth benefit. The medium S_s and F_r provided a good balance between maximizing chip removal per unit time and maintaining tool stability. Higher S_s and F_r might lead to faster M_{rr} but at the cost of faster tool wear or deflections, ultimately reducing overall M_{rr} in T51603.

Table 7: Optimized parameters – M_{rr}.

S_s	C_{fr}	D_c	F_r	M_{rr}
1750	8	0.6	750	1.3328

3.3. RSM for P_c

P_c can be measured by theoretical method and by calculation of instantenous power during machining. In the case of theoretical approach, the following equation 3 is used

$$P_c = (D_c \times W_c \times F_r \times K_c)/(60 \times 10^6) \quad (3)$$

where, W_c is the width of cut, K_c is the specific cutting force in N/mm^2.

In the case of calculation of instantenous power, forces and moments are measured with the help of Kistler dynamometer. The measured values are then compared with force and moments measured with QZZ2 dynamometer. In this study, P_c is determined using dynamometer.

According to the analysis shown in Table 8, "F-value" of 565600.00 and a "P-value" less than 0.0001 adheres to the desirability function as shown in Table 8. The insignificance of the model arises when the values records more than 0.10. In other words, only 0.01% chance exists that noise will have a negligible influence. Additionally, R^2, Adj R^2, and Pred R^2 values near to 1 justifies the efficiency of the model [20, 30, 32]. The connection between the machining parameters and P_c is clearly seen in the interaction graphs below.

3.3.1. Parameter interaction effects

The interaction effect on P_c is interpreted in the following figures. Figure 11 displays the impact of S_s and D_c on P_c. When D_c is increased while other parameters are held constant, as seen in experimental runs 8 and 9, 12 and 22, and 11 and 15, P_c increases quickly. This demonstrates that increasing parameter D_c will increase cutting force and increase power consumption. On the other hand, when parameter S_s level is altered in experimental runs 12, 15, and 17 while all other parameters are held constant, a rise in P_c is seen. However, compared to parameter D_c, the effect on power usage is a little less significant. The impact of D_c & F_r on P_c is shown in Figure 12. When F_r alone is varied as seen in experimental runs 4, 5, and 29, P_c increases quickly. This shows that the large fluctuations in cutting forces caused by a rise in parameter F_r significantly increase power usage. However, in runs 8, 9, and 26, S_s is altered while all other parameters are given fixed values. The experimental results showed that S_s directly impacts power consumption followed by D_c and F_r.

The influence of C_{fr} & F_r on P_c is depicted in Figure 13. When other parameters are held constant, the effects of parameter C_{fr} are clearly shown in the experimental runs 8 and 13, 18 and 28, 23 and 26, and so on. An incremental rise in P_c is seen in the afore mentioned runs. This validates that in this study C_{fr} makes a very

Table 8: ANOVA – P_c.

ANOVA - P_c						
SOURCE	**SS**	**df**	**MS**	**F-VALUE**	**P-VALUE**	
Model	2.97976	4	0.756819	565600.00	<0.0001	significant
A	0.078944	1	0.078957	514466.00	<0.0001	
B	2.576728	1	2.575628	637800.00	<0.0001	
C	0.236876	1	0.236877	507666.00	<0.0001	
D	0.10211008	1	0.102130	46790.00	<0.0001	
Residual Error	3.84833	24	0			
Lack of Fit	0	20	0			
Pure Error	0	4	0			
Cor Total	2.9798794	28				

Standard Deviation	0.0016565	R^2	0.984776
Mean	0.57544	Adj R^2	0.959264
C.V.%	0.0866287	Pred R^2	NA
PRESS	NA	Adequate Precision	3152.5149

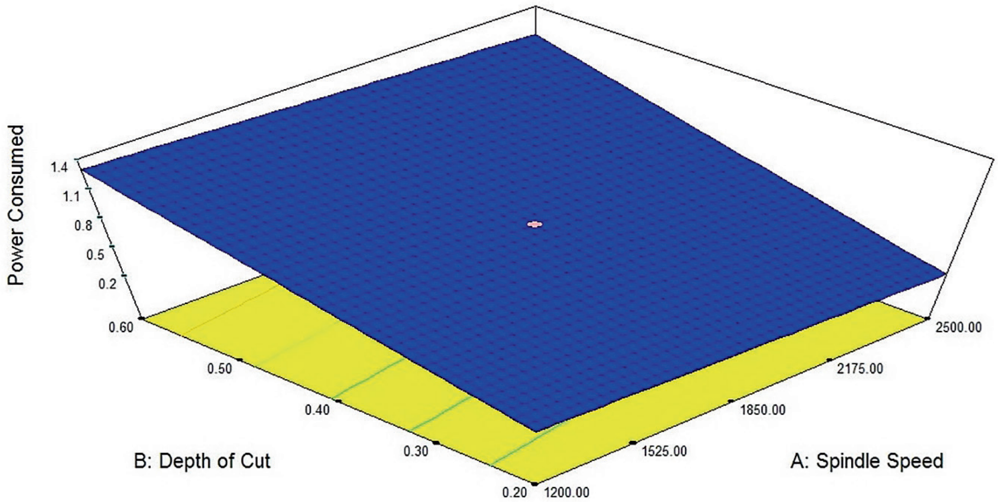

Figure 11: Interaction plot: S_s & D_c on P_c.

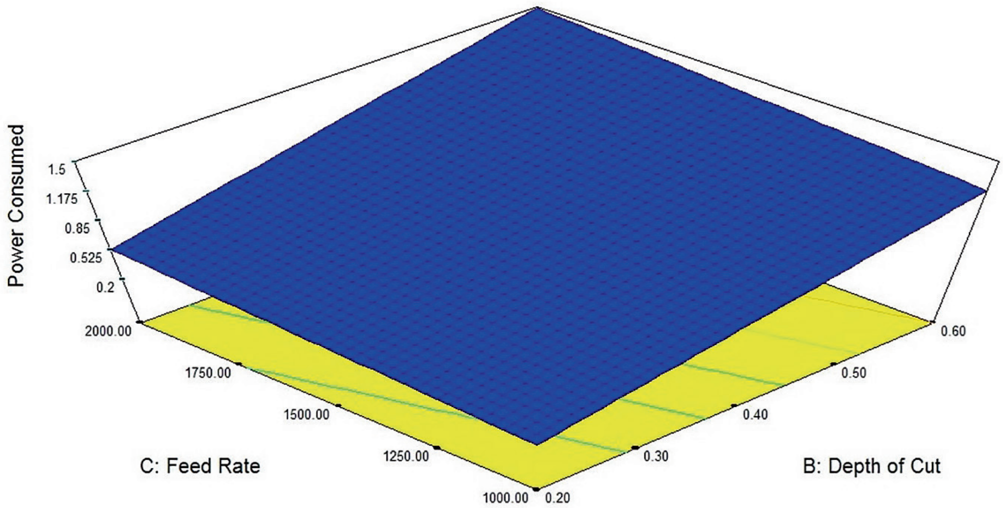

Figure 12: Interaction plot: F_r & D_c on P_c.

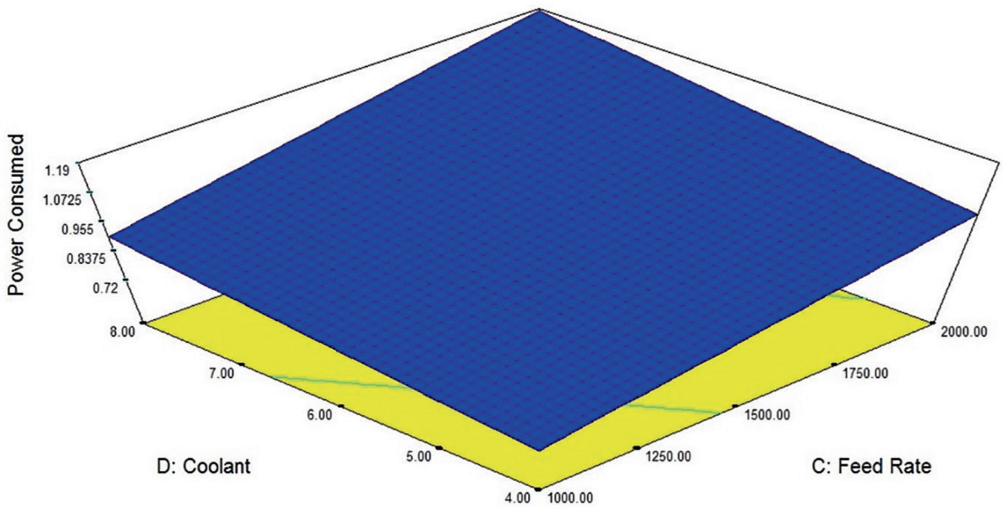

Figure 13: Interaction plot: C_{fr} & F_r on P_c.

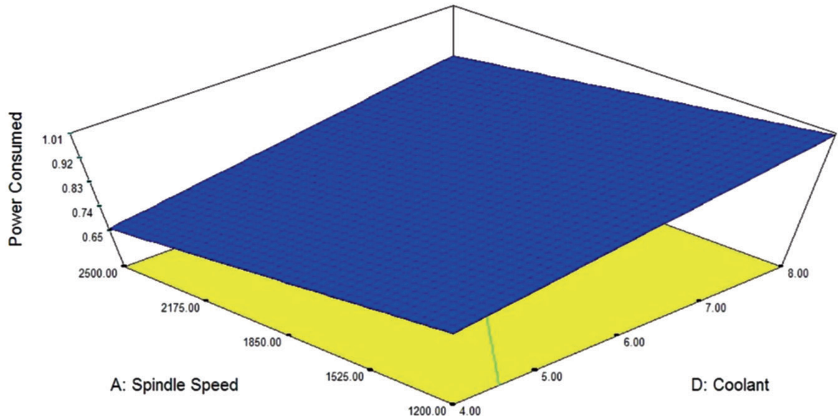

Figure 14: Interaction plot: S_s & C_{fr} on P_c.

Table 9: Optimized parameters – P_c.

S_s	D_c	F_r	C_{fr}	P_c
1750	0.2	500	6	0.205

small difference in reducing power use. On the other hand, it is noted that an increase in F_r raises P_c in runs 3 & 6, 17 & 28. The influence of S_s and C_{fr} is shown in Figure 14. Runs (8, 13), (18, 28), and (23, 26) clearly show the effect of C_{fr}. In the afore mentioned experimental runs, it was found that coolant behaviour varied according to how many other parameters were combined. On the other hand, when S_s is increased, Pc decreases in experimental runs 11 and 22, 3 and 29, and 14 and 20.

3.3.2. Predicted optimized set for P_c

Optimized level of parameters for P_c is given in Table 9 below. The medium S_s found the best relationship between minimizing friction and maximizing chip removal per unit energy. Alongside, Lower D_c and F_r directly reduce cutting forces and chip removal rate, consequently minimizing P_c. Also, lower cutting forces and temperatures at these settings likely resulted in less tool wear, further reducing P_c by maintaining cutting efficiency. Additionally, lower friction allowed for lower to medium coolant flow rates, contributing to energy savings.

4. GRA OPTIMIZATION

a) **Response Normalization:** Pre-processing of the data carried out in accordance with the established objective function. If the "large-the-better" principle is used in the normalization, then equation 4 is used for arriving at the results. If the "smaller-the-better" principle is used, then equation 5 is used. By minimizing the amount of variation from the original collection of data, normalization creates a comparable data set for easier investigation.

$$Zi(\iota) = \frac{zi(\iota) - \min zi(\iota)}{\max zi(\iota) - \min zi(\iota)} \tag{4}$$

$$Zi(\iota) = \frac{\max zi(y) - zi(y)}{\max zi(y) - \min zi(y)} \tag{5}$$

where,

m – number of data

n – responses

max $zi(\iota)$ – highest value of $zi(\iota)$

min $zi(\iota)$ – lowest value

$Zi(\iota)$ – post data pre-processing value

$zi(\iota)$ – sequencing data, original

b) Deviation Sequence Computation: For S_r and P_c "Smaller-the-better" option and "Larger-the-better" for M_{rr} is opted [24, 25]. Based on the stated condition, the normalized value deviation is calculated and recorded.

c) GRC: The following equation 6 is used for computing GRC

$$\gamma i(y) = \frac{\Delta \min + \psi \ \Delta \max}{\Delta oi(k) + \psi \ \Delta \max} \tag{6}$$

where,

$\gamma i(y)$ – grey relational coefficient

Δmin – minimum value of absolute differences

Δmin – maximum value of absolute differences

ψ – 0.5 coefficient usually ranges from 0 to 1.

d) GRD: Correlation level is performed through GRD (€). This is unique as it helps in converting a multi-response functional objective to a single function as per the equation 7.

$$€i = 1/n \sum\nolimits_{(y=1)}^{n} \gamma i(y) \tag{7}$$

4.1. Parameter optimization

Ranking is performed in this stage for identification of optimized solution. The highest rank is taken as the optimized solution. GRA executed is highlighted in Table 10.

4.2. GRA optimized result

Table 10 shows that 4th experimental run scores the highest rank and it represents the optimal sequence of parameters. In the case of multi objective optimization, higher S_s resulted in lower S_r through minimized shearing effect offering better M_{rr}, while addressing potential trade-offs with P_c and tool wear. Lower D_c supported the process by reducing the cutting forces, contributing to lower P_c and potentially smoother surfaces. Medium F_r represented a balanced role between chip formation and tool engagement, influencing both S_r and M_{rr} without incurring excessive P_c or tool wear thereby providing the optimized results was given in Table 11.

4.3. SEM image analysis for GRA

Figure 15 shows the SEM images of four different experimental runs conducted closer to the multi-objective optimized parameters arrived by GRA. Figure 15(a) shows the SEM image for optimized levels viz experimental run 4 (S_s = 2000 rpm, D_c = 0.2 mm, F_r = 750 mm/min, C_{fr} = 6 l/min).

The confirmatory run shows average S_r = 2.867 µm, P_c = 0.231 HP and M_{rr} = 0.278 IPM. The image shows presence of burrs due to hardness of the work material. During the progress of machining process, as the cutting tool wears down at faster rate continuously, it becomes less sharp and starts to tear or scrape at the material instead of cleanly shearing it. This tearing action often leaves behind small fragments of material as burrs. Moreover, when higher levels are assigned, it results in higher cutting force paving way for deformation of material at faster rate leading to tear resulting in burr formation as seen in the images. The SEM images also shows reduction in burrs cutting forces are maintained at steady pace.

In few areas smeared materials could be found may be due to lower thermal conductivity of the material. Figure 15(b) shows the SEM image experimental run 20 (S_s = 1750 rpm, D_c = 0.2 mm, F_r = 500 mm/min, C_{fr} = 6 l/min). The confirmatory run shows average S_r = 4.211 µm, P_c = 0.218 HP and M_{rr} = 0.2411 IPM. The image shows presence of burrs, adhered chip particles and smeared materials compared to Figure 15(a). Due to reduction of S_s and F_r (maintained at level 2) increased the S_r significantly. Smeared materials are also known as glazing occurs due to rubbing action of the deformed material on to the tool surface affecting the surface texture. The experimental runs and SEM images clearly shows that the formation of smeared materials is significantly influenced by nature of tool followed by F_r and D_c. Higher the levels higher are the chances of formation of smeared materials. Figure 15(c) shows the SEM image experimental run 2 (S_s = 1750 rpm, D_c = 0.2 mm, F_r = 750 mm/min, C_{fr} = 4 l/min). The confirmatory run shows average S_r = 4.641 µm, P_c = 0.261 HP and M_{rr} = 0.2123 IPM. The image shows formation of more burrs, and smeared materials along with smeared materials. The reduction in C_{fr} resulted in reduced removal of material during machining resulting in enhanced formation of smeared materials and adhered chip particles. Moreover, tearing also known as chip tearing or gouging, occurs when the material is ripped instead of being cleanly sheared off by the cutting tool leading to uneven

Table 10: GRA.

NORMALIZED VALUES			DEVIATION SEQUENCE			GREY RELATION COEFFICIENTS			GREY RELATIONAL GRADE	RANK
S_r	P_C	M_{rr}	S_r	P_C	M_{rr}	S_r	P_C	M_{rr}		
0.641	0.107	0.177	0.359	0.893	0.823	0.582	0.359	0.378	0.440	24
0.181	1.000	0.950	0.819	0.000	0.050	0.379	1.000	0.910	0.763	3
0.500	0.500	0.463	0.500	0.500	0.537	0.500	0.500	0.482	0.494	14
0.653	**0.980**	**0.941**	**0.347**	**0.020**	**0.059**	**0.590**	**0.962**	**0.894**	**0.815**	**1**
0.347	0.020	–0.014	0.653	0.980	1.014	0.434	0.338	0.330	0.367	29
0.500	0.500	0.463	0.500	0.500	0.537	0.500	0.500	0.482	0.494	14
0.206	0.413	0.271	0.794	0.587	0.729	0.386	0.460	0.407	0.418	27
0.972	0.480	0.453	0.028	0.520	0.547	0.946	0.490	0.478	0.638	6
0.000	0.877	0.799	1.000	0.123	0.201	0.333	0.803	0.713	0.617	7
0.500	0.500	0.463	0.500	0.500	0.537	0.500	0.500	0.482	0.494	14
0.613	0.464	0.503	0.387	0.536	0.497	0.564	0.483	0.502	0.516	13
0.322	0.607	0.665	0.678	0.393	0.335	0.425	0.560	0.599	0.528	12
0.706	0.036	–0.064	0.294	0.964	1.064	0.630	0.341	0.320	0.430	25
0.500	0.500	0.463	0.500	0.500	0.537	0.500	0.500	0.482	0.494	14
0.528	0.143	0.137	0.472	0.857	0.863	0.515	0.368	0.367	0.417	28
1.000	0.123	0.127	0.000	0.877	0.873	1.000	0.363	0.364	0.576	11
0.028	0.520	0.473	0.972	0.480	0.527	0.340	0.510	0.487	0.446	23
0.681	0.623	0.615	0.319	0.377	0.385	0.611	0.570	0.565	0.582	10
0.472	0.857	0.789	0.528	0.143	0.211	0.486	0.778	0.703	0.656	4
0.294	0.964	0.991	0.706	0.036	0.009	0.415	0.933	0.982	0.777	2
0.794	0.587	0.654	0.206	0.413	0.346	0.708	0.548	0.591	0.616	8
0.359	0.893	0.749	0.641	0.107	0.251	0.438	0.824	0.666	0.643	5
0.819	0.000	–0.025	0.181	1.000	1.025	0.734	0.333	0.328	0.465	21
0.387	0.536	0.423	0.613	0.464	0.577	0.449	0.519	0.464	0.477	20
0.859	0.516	0.413	0.141	0.484	0.587	0.780	0.508	0.460	0.583	9
0.319	0.377	0.311	0.681	0.623	0.689	0.423	0.445	0.420	0.430	26
0.500	0.500	0.463	0.500	0.500	0.537	0.500	0.500	0.482	0.494	14
0.678	0.393	0.262	0.322	0.607	0.738	0.608	0.452	0.404	0.488	19
0.141	0.484	0.513	0.859	0.516	0.487	0.368	0.492	0.506	0.456	22

Table 11: Optimized parameter – GRA.

S_s	D_c	F_r	C_{fr}
2000	0.2	750	6

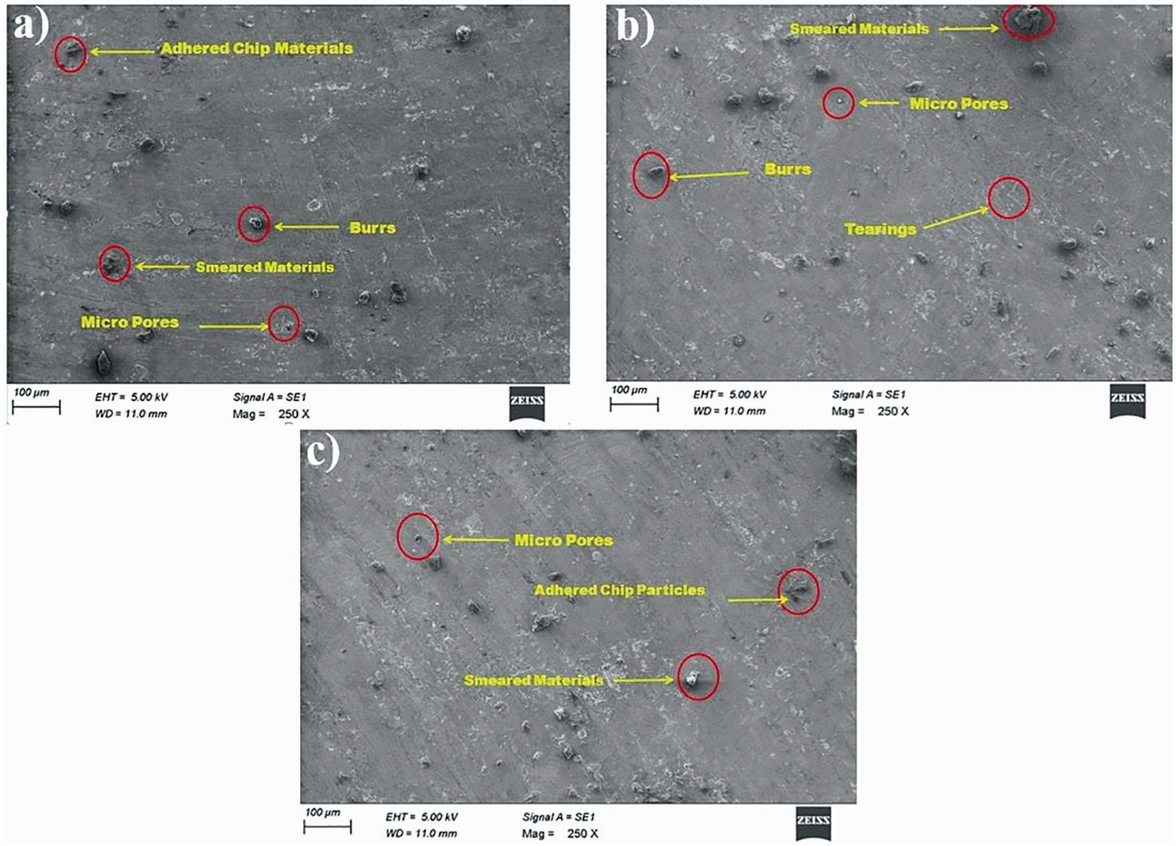

Figure 15: SEM images a) experimental run 2; b) experimental run 4; c) experimental run 20.

surfaces with poor accuracy. Micro fractures and localized stresses arising during higher level machining leads to formation of micro pores. Presence of micro pores provides more surface area for contaminants and corrosive agents to attach, potentially leading to faster degradation and decreased lifespan. Also these pores acts as stress concentration points resulting in weakening of the material and making it susceptible to failure under load.

5. CONFIRMATORY RUNS

The optimized values attained by BBD and GRA are validated through confirmatory runs to establish the deviation amid the predicted and achieved values as shown in Table 12.

Table 12: Confirmatory runs.

OPTIMIZATION TOOL	S_s	D_c	F_r	C_{fr}	PREDICTED	ACHIEVED	PREDICTED	ACHIEVED	PREDICTED	ACHIEVED
					S_r		M_{rr}		P_c	
BOX BEHNKEN - SINGLE OBJECTIVE										
S_r	2000	0.6	750	6	1.524	1.568	–	–	–	–
M_{rr}	1750	0.6	750	8	–	–	1.3328	1.4335	–	–
Deviation					**S_s = 0.044**		**M_{rr} = 0.101**		–	–
% Deviation					**S_s = 2.89**		**M_{rr} = 7.55**		–	–
MULTI-OBJECTIVE										
P_c	1750	0.2	500	6	4.207	3.807	0.2351	0.2678	0.205	0.231
Deviation					**S_s = 0.4**		**M_{rr} = 0.0327**		**P_c = 0.026**	
% Deviation					**S_s = 9.5**		**M_{rr} = 13.91**		**P_c = 12.68**	
GRA – MULTI OBJECTIVE										
S_s/M_{rr}/P_c	2000	0.2	750	6	2.844	2.867	0.262	0.278	0.2171	0.2201
Deviation					**S_s = 0.023**		**M_{rr} = 0.016**		**P_c = 0.003**	
% Deviation					**S_s = 0.81**		**M_{rr} = 6.1**		**P_c = 1.38**	

6. CONCLUSIONS

In CNC end milling, the low-carbon mold steel is subjected to parameter optimization. S_s, M_{rr}, P_c, were optimized. The following findings from this experimental analysis are deemed to be noteworthy:

1. The lowest S_r was achieved using the following parameters: 2000 rpm, 0.6 mm, 750 mm/min, and 6 l/min.
2. Achieved least P_c at 1750 rpm, 0.2 mm, 500 mm/min, and 6 l/min.
3. The maximum M_{rr} was achieved using the following parameters: 1750 rpm, 0.6 mm, 750 mm/min, and 8 l/min.
4. Each of the afore mentioned settings are true as long as it is viewed as a single response.
5. Using the box-Behnken design, the multi-objective optimal level was attained at 1750 rpm, 0.2 mm, 500 mm/min, and 6 l/min.
6. According to GRA, optimized result was achieved at 2000 rpm, 0.2 mm, 750 mm/min, and 6 l/min.
7. The usage of coolant between low to medium level serves as a strong recommendation towards sustainable practice as minimized usage of coolant leads to lesser environmental impact.
8. Both optimization strategies are found to be efficient and can be taken into consideration for machining as long as the percentage deviation is less than 10%.

6.1. Future scope of work

1. The above work can be further extended applying the concepts of different green machining techniques addressing sustainable practice.
2. Different tools can be considered for study to evaluate multi-objective optimization involving contradictory responses.
3. Condition monitoring principles can be applied to govern the optimized parameters through closed feedback loop.

7. ACKNOWLEDGMENT

This project is funded by DST-FIST (2022), Government of India vide Ref. No: SR/FST/College-/2022/1300.

8. BIBLIOGRAPHY

[1] WANG, M.Y., CHANG, H.Y., “Experimental study of surface roughness in slot end milling AL2014-T6”, *International Journal of Machine Tools & Manufacture*, v. 44, n. 1, pp. 51–57, Jan. 2004. doi: http://dx.doi.org/10.1016/j.ijmachtools.2003.08.011.

[2] PALANISAMY, P., RAJENDRAN, I., SHANMUGASUNDARAM, S., “Optimization of machining parameters using genetic algorithm and experimental validation for end-milling operations”, *International Journal of Advanced Manufacturing Technology*, v. 32, n. 7–8, pp. 644–655, Apr. 2007. doi: http://dx.doi.org/10.1007/s00170-005-0384-3.

[3] MUTHUKRISHNAN, N., DAVIM, J.P., “Optimization of machining parameters of Al/SiC-MMC with ANOVA and ANN analysis”, *Journal of Materials Processing Technology*, v. 209, n. 1, pp. 225–232, Jan. 2009. doi: http://dx.doi.org/10.1016/j.jmatprotec.2008.01.041.

[4] QUINTANA, G., CIURANA, J.D., RIBATALLADA, J., “Surface roughness generation and material removal rate in ball end milling operations”, *Materials and Manufacturing Processes*, v. 25, n. 6, pp. 386–398, May. 2010. doi: http://dx.doi.org/10.1080/15394450902996601.

[5] MANSOUR, A., ABDALLA, H., “Surface roughness model for end milling: a semi-free cutting carbon casehardening steel (EN32) in dry condition”, *Journal of Materials Processing Technology*, v. 124, n. 1–2, pp. 183–191, Jun. 2002. doi: http://dx.doi.org/10.1016/S0924-0136(02)00135-8.

[6] SURESH, K.R., SENTHIL, K.S., MURUGAN, K., *et al*., “Green machining characteristics study of Al-6063 in CNC milling using Taguchi method and grey relational analysis”, *Advances in Materials Science and Engineering*, v. 2021, pp. 1–12, Dec. 2021. doi: http://dx.doi.org/10.1155/2021/4420250.

[7] CHANG, H.K., KIM, J.H., KIM, I.H., *et al*., “In-process surface roughness prediction using displacement signals from spindle motion”, *International Journal of Machine Tools & Manufacture*, v. 47, n. 6, pp. 1021–1026, May 2007. http://dx.doi.org/10.1016/j.ijmachtools.2006.07.004.

[8] GOLOGLU, C., SAKARYA, N., “The effects of cutter path strategies on surface roughness of pocket milling of 1.2738 steel based on Taguchi method”, *Journal of Materials Processing Technology*, v. 206, n. 1–3, pp. 7–15, Sep. 2008. doi: http://dx.doi.org/10.1016/j.jmatprotec.2007.11.300.

[9] DHOKIA, V.G., KUMAR, S., VICHARE, P., *et al*., "An intelligent approach for the prediction of surface roughness in ball-end machining of polypropylene", *Robotics and Computer-integrated Manufacturing*, v. 24, n. 6, pp. 835–842, Dec. 2008. doi: http://dx.doi.org/10.1016/j.rcim.2008.03.019.

[10] VISWANATHAN, R., RAMESH, S., MANIRAJ, S., *et al*., "Measurement and multi-response optimization of turning parameters for magnesium alloy using hybrid combination of Taguchi-GRA-PCA technique", *Measurement*, v. 159, pp. 107800, Jul. 2020. doi: http://dx.doi.org/10.1016/j.measurement.2020.107800.

[11] ABU-MAHFOUZ, I., BANERJEE, A., RAHMAN, E., "Evolutionary optimization of machining parameters based on surface roughness in end milling of hot rolled steel", *Materials (Basel)*, v. 14, n. 19, pp. 5494, Sep. 2021. doi: http://dx.doi.org/10.3390/ma14195494. PubMed PMID: 34639893.

[12] VISHNU, V.S., VARGHESE, K.G., GURUMOORTHY, B., "A data-driven digital twin of CNC machining processes for predicting surface roughness", *Procedia CIRP*, v. 104, pp. 1065–1070, Jan. 2021. doi: http://dx.doi.org/10.1016/j.procir.2021.11.179.

[13] SAVKOVIC, B., KOVAC, P., RODIC, D., *et al*., "Comparison of artificial neural network, fuzzy logic and genetic algorithm for cutting temperature and surface roughness prediction during the face milling process", *Advances in Production Engineering & Management*, v. 15, n. 2, pp. 137–150, Jun. 2020. doi: http://dx.doi.org/10.14743/apem2020.2.354.

[14] SURYARAJ, G.K., PRINCE, M., MANIRAJ, J., "Optimization of boriding process on AISI 1015 steel using response surface methodology", *Matéria (Rio de Janeiro)*, v. 28, n. 2, pp. e20230086, Jun. 2023. doi: http://dx.doi.org/10.1590/1517-7076-rmat-2023-0086.

[15] NADALE, H.C., SVOBODA, H.G., "Fatigue life of PAW welded joints of high strength microalloyed boron steels", *Matéria (Rio de Janeiro)*, v. 23, n. 2, pp. e11996, 2018.

[16] ANAND, T., RAGUPATHY, K., RANGANATHAN, L., "Optimization of drilling parameters using GRA for polyamide 6 nanocomposites", *Matéria (Rio de Janeiro)*, v. 28, n. 2, pp. e20220337, May 2023. doi: http://dx.doi.org/10.1590/1517-7076-rmat-2022-0337.

[17] PANWAR, V., SHARMA, D.K., KUMAR, K.P., *et al*., "Experimental investigations and optimization of surface roughness in turning of en 36 alloy steel using response surface methodology and genetic algorithm", *Materials Today: Proceedings*, v. 46, pp. 6474–6481, Jan. 2021. doi: http://dx.doi.org/10.1016/j.matpr.2021.03.642.

[18] ZAHOOR, S., AZAM, H.A., MUGHAL, M.P., *et al*., "WEDM of complex profile of IN718: multi-objective GA-based optimization of surface roughness, dimensional deviation, and cutting speed", *International Journal of Advanced Manufacturing Technology*, v. 114, n. 7–8, pp. 2289–2307, Jun. 2021. doi: http://dx.doi.org/10.1007/s00170-021-06916-8.

[19] OKTEM, H., ERZURUMLU, T., ERZINCANLI, F., "Prediction of minimum surface roughness in end milling mold parts using neural network and genetic algorithm", *Materials & Design*, v. 27, n. 9, pp. 735–744, Jan. 2006.

[20] SINGH, T., SHARMA, V.K., RANA, M., *et al*., "Multi response optimization of process variables in MQL assisted face milling of EN31 alloy steel using grey relational analysis", *Materials Today: Proceedings*, v. 47, pp. 4062–4066, Jan. 2021. doi: http://dx.doi.org/10.1016/j.matpr.2021.05.408.

[21] SHAIKH, M.B.N., ALI, M., KHAN, Z.A., *et al*., "An MCDM approach for multi-response optimisation of machining parameters in turning of EN8 steel (AISI-1040) for sustainable manufacturing", *International Journal on Interactive Design and Manufacturing*, v. 17, n. 6, pp. 3159–3176, Jun. 2023. doi: http://dx.doi.org/10.1007/s12008-023-01368-8.

[22] MIAN, T., MAGO, J., SHAIKH, M.B.N., *et al*., "Near dry turning of EN8 and EN31 steel: multi-objective optimization using grey relational analysis", *Engineering Research Express*, v. 4, n. 3, pp. 035053, Sep. 2022. doi: http://dx.doi.org/10.1088/2631-8695/ac90a0.

[23] SHAIKH, M.B.N., ALI, M., "Turning of steels under various cooling and lubrication techniques: a review of literature, sustainability aspects, and future scope", *Engineering Research Express*, v. 3, n. 4, pp. 042001, Nov. 2021. doi: http://dx.doi.org/10.1088/2631-8695/ac2e10.

[24] JOEL, C., JEYAPOOVAN, T., "Optimization of machinability parameters in abrasive water jet machining of AA7075 using Grey-Taguchi method", *Materials Today: Proceedings*, v. 37, pp. 737–741, Jan. 2021. doi: http://dx.doi.org/10.1016/j.matpr.2020.05.741.

[25] BELLUBBI, S., SATHISHA, N., MALLICK, B., "Multi response optimization of ECDM process parameters for machining of microchannel in silica glass using Taguchi-GRA technique", *Silicon*, v. 14, n. 8, pp. 4249–4263, Jun. 2022. doi: http://dx.doi.org/10.1007/s12633-021-01167-4.

[26] BAI, L., CHENG, X., YANG, Q., *et al*., "Predictive model of surface roughness in milling of 7075Al based on chatter stability analysis and back propagation neural network", *International Journal of Advanced Manufacturing Technology*, v. 126, n. 3-4, pp. 1347–1361, May 2023. doi: http://dx.doi.org/10.1007/s00170-023-11133-6.

[27] TLHABADIRA, I., DANIYAN, I.A., MASU, L., *et al*., "Process design and optimization of surface roughness during M200 TS milling process using the Taguchi method", *Procedia CIRP*, v. 84, pp. 868–873, Jan. 2019. doi: http://dx.doi.org/10.1016/j.procir.2019.03.200.

[28] FEDAI, Y., KAHRAMAN, F., KIRLI, A.K.I.N., *et al*., "Optimization of machining parameters in face milling using multi-objective Taguchi technique", *Technical Journal*, v. 12, n. 2, pp. 104–108, Jun. 2018.

[29] MOGANAPRIYA, C., RAJASEKAR, R., SATHISH KUMAR, P., *et al*., "Achieving machining effectiveness for AISI 1015 structural steel through coated inserts and grey-fuzzy coupled Taguchi optimization approach", *Structural and Multidisciplinary Optimization*, v. 63, n. 3, pp. 1169–1186, Mar. 2021. doi: http://dx.doi.org/10.1007/s00158-020-02751-9.

[30] VENKATESH, S., KUMAR, R.S., SIVAPIRAKASAM, S.P., *et al*., "Multi-objective optimization, experimental and CFD approach for performance analysis in square cyclone separator", *Powder Technology*, v. 371, pp. 115–129, Jun. 2020. doi: http://dx.doi.org/10.1016/j.powtec.2020.05.080.

[31] SRINIVASAN, A., PRABU, R., RAMESH, S., *et al*., "Investigation and optimization on micro and nano Al2O3 reinforced aluminium composites using GRA coupled PCA technique", *Journal of Ceramic Processing Research*, v. 23, n. 6, pp. 783–793, Dec. 2022.

[32] RAVIKUMAR, N., VIJAYAN, R., VISWANATHAN, R., "Multi-response optimisation for turning of magnesium alloy with untreated and cryogenic treated carbide inserts by grey relational analysis", *Journal of Ceramic Processing Research*, v. 24, n. 1, pp. 142–152, Feb. 2023.